

Satellite-based Estimation of the Impacts of Summertime Wildfires on $PM_{2.5}$ in United States

Zhixin Xue¹, Pawan Gupta^{2,3}, and Sundar Christopher¹

¹Department of Atmospheric and Earth Science, The University of Alabama in Huntsville, Huntsville, 35806 AL, USA

²STI, Universities Space Research Association (USRA), Huntsville, 35806 AL, USA

³NASA Marshall Space Flight Center, Huntsville, AL, 35806, USA

Abstract

Frequent and widespread wildfires in North Western United States and Canada has become the “*new normal*” during the northern hemisphere summer months, which significantly degrades particulate matter air quality in the United States. Using the mid-visible Multi Angle Implementation of Atmospheric Correction (MAIAC) satellite-derived Aerosol Optical Depth (AOD) with meteorological information from the European Centre for Medium-Range Weather Forecasts (ECMWF) and other ancillary data, we quantify the impact of these fires on fine particulate matter ($PM_{2.5}$) air quality in the United States. We use a Geographically Weighted Regression method to estimate surface $PM_{2.5}$ in the United States between low (2011) and high (2018) fire activity years. Our results indicate that smoke aerosols caused significant pollution changes over half of the United States. We estimate that nearly 29 states have increased $PM_{2.5}$ during the fire active year and 15 of these states have $PM_{2.5}$ concentrations more than 2 times than that of the inactive year. Furthermore, these fires increased daily mean surface $PM_{2.5}$ concentrations in Washington and Oregon by 38 to $259\mu\text{g}\text{m}^{-3}$ posing significant health risks especially to vulnerable populations. Our results also show that the GWR model can be

Deleted: Particulate Matter Air Quality

Deleted:

Formatted: Subscript

Formatted: Subscript

Formatted: Subscript

Formatted: Subscript

Formatted: Subscript

Xue, Gupta, Christopher, submitted to [Atmospheric Chemistry and Physics Discussion](#)

25 successfully applied to $PM_{2.5}$ estimations from wildfires thereby providing useful information for
26 various applications including public health assessment.

Formatted: Subscript

27 1. Introduction

28 The United States (US) Clean Air Act (CAA) was passed in 1970 to reduce pollution levels
29 and protect public health that has led to significant improvements in air quality (Hubbell et al.,
30 2010; Samet, 2011). However, the northern part of the US continues to experience an increase in
31 surface $PM_{2.5}$ due to fires in North Western United States and Canada (hereafter NWUSC)
32 especially during the summer months and these aerosols are a new source of 'pollution' (Coogan
33 et al., 2019; Dreessen et al., 2016). The smoke aerosols from these fires increase fine particulate
34 matter ($PM_{2.5}$) concentrations and degrade air quality in the United States (Miller et al., 2011).
35 Moreover, several studies have shown that from 2013 to 2016, over 76% of Canadians and 69%
36 of Americans were at least minimally affected by wildfire smoke (e.g. Munoz-Alpizar et al., 2017).
37 Although wildfire pre-suppression and suppression costs have increased, the number of large fires
38 and the burnt areas in many parts of western Canada and the United States have also increased.
39 (Hanes et al., 2019; Tymstra et al., 2019). Furthermore, in a changing climate, as surface
40 temperature increases and humidity decreases, the flammability of land cover also increases, and
41 thus accelerate the spread of wildfires (Melillo et al., 2014). The accumulation of flammable
42 materials like leaf litter can potentially trigger severe wildfire events even in those forests that
43 hardly experience wildfires (Calkin et al., 2015; Hessburg et al., 2015; Stephens, 2005).

Formatted: Subscript

Formatted: Subscript

44 Wildfire smoke exposure can cause small particles to be lodged in lungs that may lead to
45 exacerbations of asthma chronic obstructive pulmonary disease (COPD), bronchitis, heart disease
46 and pneumonia (Apte et al., 2018; Cascio, 2018). According to a recent study, a $10 \mu g m^{-3}$
47 increase in $PM_{2.5}$ is associated with a 12.4% increase in cardiovascular mortality (Kollanus et al.,

Formatted: Subscript

Xue, Gupta, Christopher, submitted to [Atmospheric Chemistry and Physics Discussion](#)

48 2016). In addition, exposure to wildfire smoke is also related to massive economic costs due to
49 premature mortality, loss of workforce productivity, impacts on the quality of life and
50 compromised water quality (Meixner and Wohlgemuth, 2004).

51 Surface $PM_{2.5}$ is one of the most commonly used parameters to assess the health effects of
52 ambient air pollution. Given the sparsity of measurements in many parts of the world, it is not
53 possible to use interpolation techniques between monitors to provide $PM_{2.5}$ estimate on a square
54 kilometer basis. Since surface monitors are limited, satellite data has been used with numerous
55 ancillary data sets to estimate surface $PM_{2.5}$ at various spatial scales. Several techniques have been
56 developed to estimate surface $PM_{2.5}$ using satellite observations from regional to global scales
57 including simple linear regression, multiple linear regression, mixed-effect model, chemical
58 transport model (scaling methods), geographically weighted regression (GWR), and machine
59 learning methods (see Hoff and Christopher, 2009 for a review). The commonly used global
60 satellite data product is the 550nm (mid-visible) aerosol optical depth (AOD) which is a unitless
61 columnar measure of aerosol extinction. Simple linear regression methods use satellite AOD as
62 the only independent variable, which shows limited predictability compared to other methods and
63 correlation coefficients vary from 0.2 to 0.6 from the Western to Eastern United States (Zhang et
64 al., 2009). Multiple linear regression method uses meteorological variables along with AOD data,
65 and the prediction accuracy varies with different conditions including the height of boundary layer
66 and other meteorological conditions (Goldberg et al., 2019; Gupta and Christopher, 2009b; Liu et
67 al., 2005). For both univariate model and multi-variate models, AOD shows stronger correlation
68 with $PM_{2.5}$ during-fire episodes compared to pre-fire and post-fire periods (Mirzaei et al., 2018).
69 Chemistry transport models (CTM) that scale the satellite AOD by the ratio of $PM_{2.5}$ to AOD
70 simulated by models can provide $PM_{2.5}$ estimations without ground measurements, which are

Formatted: Subscript

Formatted: Subscript

Formatted: Subscript

Formatted: Subscript

Deleted: s

Formatted: Subscript

Formatted: Subscript

Formatted: Subscript

Xue, Gupta, Christopher, submitted to [Atmospheric Chemistry and Physics Discussion](#)

72 different than other statistical methods (Donkelaar et al., 2019, 2006). However, the CTM models
73 that depend on reliable emission data usually show limited predictability at shorter time scales,
74 and is largely useful for studies that require annual averages (Hystad et al., 2012).

75 The relationship among $PM_{2.5}$, AOD and other meteorological variables is not spatially
76 consistent (Hoff and Christopher, 2009; Hu, 2009). Therefore, methods that consider spatial
77 variability can replicate surface $PM_{2.5}$ with higher accuracy. One such method is the GWR, which
78 is a non-stationary technique that [accounts for](#) spatially varying relationships by assuming [that](#) the
79 coefficients in the model are functions of locations (Brunsdon et al., 1996; Fotheringham et al.,
80 1998, 2003). In 2009, satellite-retrieved AOD was introduced in the GWR method to predict
81 surface $PM_{2.5}$ (Hu, 2009) followed by the use of meteorological parameters and land use
82 information (Hu et al., 2013). [Meteorological variables are crucial for simulating surface \$PM_{2.5}\$](#)
83 [since they interact with \$PM_{2.5}\$ through different processes which will be discussed in detail in the](#)
84 [data section](#) (Chen et al., 2020). Several studies (Guo et al., 2021; Ma et al., 2014; You et al.,
85 2016) successfully applied [the](#) GWR model [for](#) estimating $PM_{2.5}$ in China by using AOD and
86 meteorological features as predictors. Similar to all the statistical methods, however, the GWR
87 relies on adequate number and density of surface measurements (Chu et al., 2016; Gu, 2019; Guo
88 et al., 2021), underscoring the importance of adequate ground monitoring of surface $PM_{2.5}$.

89 In this paper, we use satellite data from the Moderate Resolution Imaging
90 Spectroradiometer (MODIS) and surface $PM_{2.5}$ data combined with meteorological and other
91 ancillary information to develop and use the GWR method to estimate $PM_{2.5}$. The use of the GWR
92 method is not novel and we merely use a proven method to apply this towards surface $PM_{2.5}$
93 estimations for forest fires. We calculate the change in $PM_{2.5}$ between a high fire activity (2018)
94 with low fire activity (2011) periods during summer to assess the role of NWUSC wildfires on

Formatted: Subscript

Formatted: Subscript

Deleted: models

Formatted: Subscript

Deleted: in

Formatted: Subscript

Formatted: Subscript

Formatted: Subscript

Formatted: Subscript

Formatted: Subscript

Formatted: Subscript

Xue, Gupta, Christopher, submitted to [Atmospheric Chemistry and Physics Discussion](#)

97 surface $PM_{2.5}$ in the United States. The paper is organized as follows: We describe the data sets
98 used in this study followed by the GWR method. We then describe the results and discussion
99 followed by a summary with conclusions.

101 2. Data

102 A 17-day period (August 9th to August 25th) in 2018 (high fire activity) and 2011 (low fire
103 activity) was selected based on analysis of total fires (details in methodology section) to assess
104 surface $PM_{2.5}$ (Table 1).

105 **2.1 Ground level $PM_{2.5}$ observations:** Daily surface $PM_{2.5}$ from the Environment Protection
106 Agency (EPA) are used in this study. These data are from Federal Reference Methods (FRM),
107 Federal Equivalent Methods (FEM), or other methods that are to be used in the National Ambient
108 Air Quality Standards (NAAQS) decisions. A total of 1003 monitoring sites in the US are included
109 in our study with 949 having valid observations in the study period in 2018, and a total of 873 sites
110 with 820 having valid observations in the study period in 2011. $PM_{2.5}$ values less than $2 \mu\text{gm}^{-3}$ are
111 discarded since they are lower than the established detection limit (Hall et al., 2013).

112 **2.2 Satellite Data:** [AOD which represents the total column aerosol mass loading is related to](#)
113 [surface \$PM_{2.5}\$ as a function of aerosol vertical properties and physical properties \(Koelemeijer et](#)
114 [al., 2006\):](#)

$$115 \quad AOD = PM_{2.5} H f(RH) \frac{3Q_{\text{ext,dry}}}{4\rho r_{\text{eff}}} = PM_{2.5} H S \quad (1)$$

116 [Where H is the aerosol layer height, f\(RH\) is the ratio of ambient and dry extinction coefficients,](#)
117 [Q_{ext,dry} is the extinction efficiency under dry conditions, r_{eff} is the particle effective radius, ρ is the](#)

Formatted: Subscript

Formatted: Subscript

Formatted: Subscript

Formatted: Subscript

Formatted: Subscript

Field Code Changed

Formatted: Font: 12 pt

Formatted: Font: (Default) Times New Roman, 12 pt

Xue, Gupta, Christopher, submitted to [Atmospheric Chemistry and Physics Discussion](#)

118 aerosol mass density and S is the specific extinction efficiency ($\text{m}^2 \text{g}^{-1}$) of the aerosol at ambient
119 conditions. Therefore AOD usually has a strong positive correlation with $\text{PM}_{2.5}$, and the
120 relationship varies depending on other meteorological parameters which will be discussed in detail
121 in the following section.

122 The MODIS mid visible AOD from the Multi-Angle Implementation of Atmospheric Correction
123 (MAIAC) product (MCD19A2 Version 6 data product) is used in this study. We used [the MAIAC-](#)
124 retrieved Terra and Aqua MODIS AOD product at 1 km pixel resolution (Lyapustin et al., 2018).

125 Different orbits are averaged to obtain mean daily values. Since thick smoke plumes generated by
126 wildfires can be [miscalssified](#) as cloud, we preserve possible cloud contaminated pixels to preserve
127 the thick smoke pixels, and only AOD less than 0 will be discarded. Validation with AERONET
128 studies show that 66% of the MAIAC AOD data agree within $\pm 0.5 \sim \pm 0.1$ AOD (Lyapustin et al.,
129 2018). Largely due to cloud cover, grid cells may have limited number of AOD observations within
130 a certain period. On average, cloud free AOD data are available about 40% of the time during
131 August 9th to August 25th in 2018 when fires were active in the region bounded by 25~50°N,
132 65~125°W. Smoke flag from the same product is used as a predictor in estimating surface $\text{PM}_{2.5}$.

133 **The smoke detection is performed using MODIS red, blue and deep blue bands, and smoke pixels**
134 **are separated from from dust and clouds based on absorption parameter, size parameter and**
135 **thermal thresholds (see Lyapustin et al., 2018, 2012 for further discussion). Smoke flag data can**
136 **provide the percentage of smoke pixel in each grid, which is related to smoke coverage.**

137 We also use the MODIS level-3 daily FRP (MCD14ML, fire radiative power) product
138 which combines Terra and Aqua fire products to assess wildfire activity. The fire radiative energy
139 indicates the rate of combustion and thus FRP can be used for characterizing active fires (Freeborn

Deleted: the

Deleted: detected

Deleted: by a large chance

Formatted: Subscript

Xue, Gupta, Christopher, submitted to [Atmospheric Chemistry and Physics Discussion](#)

143 et al, 2014). For purposes of the study we sum the FRP within every $2.3^{\circ} \times 3.5^{\circ}$ box to represent
144 the total fire activity in different locations.

145 **2.3 Meteorological data:** Meteorological information including boundary layer height (BLH), 2m
146 temperature (T2M), 10m wind speed (WS), surface relative humidity (RH) and surface pressure
147 (SP) are obtained from the European Centre for Medium-Range Weather Forecasts (ECMWF)
148 reanalysis (ERA5) product, with a spatial resolution of 0.25 degrees and temporal resolution of 1
149 hour and is matched temporally with the satellite overpass time. [The meteorological parameters](#)
150 [provide important information of different processes affecting surface PM_{2.5} concentration, which](#)
151 [can affect the AOD-PM_{2.5} relationship as previously discussed.](#)

152 The BLH can provide information of aerosol layer height ([H in equation 1](#)) as aerosols are often
153 found to be well-mixed within the boundary layer (Gupta and Christopher, 2009b). [With same](#)
154 [amount of pollution within the boundary layer, the higher the BLH is, the more PM_{2.5} is](#)
155 [distributed within that layer and vice-versa](#) (Miao et al., 2018; Zheng et al., 2017). [Therefore,](#)
156 [PM_{2.5} usually has an anticorrelation with BLH. Surface temperature \(T2M\) can affect PM_{2.5}](#)
157 [through convection, evaporation, temperature inversion and secondary pollutant generation](#)
158 [processes \(Chen et al., 2020\). The first two processes are negatively related to PM_{2.5}](#)
159 [concentration: 1\) higher temperature increases turbulence and atmospheric convections which](#)
160 [accelerate the pollution dispersion \(PM_{2.5} decreases\); 2\) higher temperature increases loss of](#)
161 [PM_{2.5} including ammonium nitrate and other volatile or semi-volatile components](#) (Wang et al.,
162 2017). [The latter two processes are positively related to PM_{2.5} by limiting vertical motion and](#)
163 [promoting photochemical reactions under high temperature](#) (Xu et al., 2019; Zhang et al., 2015).
164 [Wind speed \(WS\) are often negatively related to PM_{2.5} since it increases the dispersion of](#)
165 [pollutants. However, unique geographical conditions \(such like mountains\) with certain wind](#)

Formatted: Font: (Default) Times New Roman, 12 pt

Formatted: Font: (Default) Times New Roman, 12 pt

Formatted: Font: (Default) Times New Roman, 12 pt

Formatted: Font: (Default) Times New Roman, 12 pt

Formatted: Font: (Default) Times New Roman, 12 pt

Formatted: Font: (Default) Times New Roman, 12 pt

Deleted: s

167 [directions can cause accumulations of pollutants](#) (Chen et al., 2017). [RH may promote](#)
168 [hygroscopic growth of particles to increase PM_{2.5}](#) (Trueblood et al., 2018; Zheng et al., 2017),
169 [but it can also reduce PM_{2.5} through the deposition process. SP may influence the diffusion or](#)
170 [accumulation of pollutants through formation of low-level wind convergence](#) (You et al.,

171 2017). **3. Methodology**

172 To assess the impact of NWUSC fires on PM_{2.5} in the United States, we first estimate the
173 PM_{2.5} over the study region during a time period with high fire activity (2018). We then use the
174 same method during a year with low fire activity (2011) to compare the differences between the
175 two years. The two years are selected based on the total FRP in August calculated within Canada
176 (49~60°N, 55~135°W) and Northwestern (NW) US (35~49°N, 105~125°W). Table 2 shows the
177 total FRP in Canada and Northwestern US in August from 2010 to 2018. The total FRP in the two
178 regions is lowest in 2011 and highest in 2018 during the 9 years, which provides the basis for the
179 study. In order to create a 0.1° surface PM_{2.5}, the GWR model is used to estimate the relationships
180 of PM_{2.5} and AOD. Detailed processing steps for GWR model are shown in Figure 1.

181 **3.1 Data preprocessing:** The first step is to resample all datasets to a uniform spatial resolution
182 by creating a 0.1° resolution grid covering the Continental United States. During this process, we
183 collocate the PM_{2.5} data and average the values if there is more than one value in one grid. Then
184 the MAIAC AOD and smoke flag are averaged into 0.1° grid cells. Meteorological datasets are
185 also resampled to the 0.1° grid cells by applying the inverse distance method.

186 **3.2 Time selecting & averaging:** Next we select data where AOD and ground PM_{2.5} are both
187 available (AOD > 0 and PM_{2.5} > 2.0 $\mu\text{g m}^{-3}$) and average them for the study period. This is to
188 ensure that the AOD, PM_{2.5} and other variables match with each other, because PM_{2.5} is not a
189 continuous measurement for some sites and AOD have missing values due to cloud cover and

Deleted: A higher RH will increase the hygroscopicity, change scattering properties of certain aerosols and can lead to a higher AOD value (Zheng et al., 2017). In addition, high surface temperatures can also accelerate the formation of secondary particles in the atmosphere. ¶

Formatted: Subscript

Formatted: Subscript

Formatted: Subscript

Formatted: Subscript

Formatted: Subscript

Formatted: Subscript

Formatted: Subscript

Formatted: Subscript

Formatted: Subscript

Xue, Gupta, Christopher, submitted to [Atmospheric Chemistry and Physics Discussion](#)

195 other reasons. Therefore, it is important to use data from days where both measurements are
196 available to avoid sampling biases.

197 **3.3 GWR model development and validation:** The Adaptive bandwidth selected by the Akaike's
198 Information Criterion (AIC) is used for the GWR model (Loader, 1999). For locations that already
199 have $PM_{2.5}$ monitors, we calculate the mean AOD of a $0.5 \times 0.5^\circ$ box centered at the ground location
200 and estimate the GWR coefficients (β) for AOD and meteorological variables to estimate $PM_{2.5}$.
201 The model structure can be expressed as:

$$202 \quad PM_{2.5i} = \beta_{0,i} + \beta_{1,i}AOD_i + \beta_{2,i}BLH_i + \beta_{3,i}T2M_i + \beta_{4,i}U10M_i + \beta_{5,i}RH_{sfci} + \beta_{6,i}SP_i + \beta_{7,i}SF_i \\ 203 \quad \quad \quad + \varepsilon_i$$

204 where $PM_{2.5i}$ ($\mu g m^{-3}$) is the selected ground-level $PM_{2.5}$ concentration at location i ; $\beta_{0,i}$
205 is the intercept at location i ; $\beta_{1,i} \sim \beta_{8,i}$ are the location-specific coefficients; AOD_i is the resampled
206 AOD selected from MAIAC daily AOD data at location i ; $BLH_i, T2M_i, U10M_i, RH_{sfci}, SP_i$ are
207 selected meteorological parameters (BLH, T2M, WS, RH and PS) at location i ; SF_i (%) is the
208 resampled smoke flag data at location i and ε_i is the error term at location i .

209 We perform the Leave One Out Cross Validation (LOOCV) to test the model predictive
210 performance (Kearns and Ron, 1999). Since the GWR model relies on adequate number of
211 observations, the prediction accuracy will be lower if we preserve too much data for validation.
212 Therefore, we choose the LOOCV method, which preserve only one data for validation at a time
213 and repeat the process until all the data are used. In addition, R^2 and RMSE are calculated for both
214 model fitting and model validation process to detect overfitting. Model overfitting will lead to low
215 predictability, which means it fits too close to the limited number of data to predict for other places
216 and will cause large bias.

Xue, Gupta, Christopher, submitted to [Atmospheric Chemistry and Physics Discussion](#)

217 **3.4 Model prediction:** While predicting the ground-level $PM_{2.5}$ for unsampled locations, we make
218 use of the estimated parameters for sites within a 5° radius to generate new slopes for independent
219 variables based on the spatial weighting matrix (Brunsdon et al., 1996). The closer to the predicted
220 location, the closer to 1 the weighting factor will be, while the weighting factor for sites further
221 than the 5° in distance is zero. It is important to note that AOD and other independent variables
222 used for prediction in this step are averaged values for days that have valid AOD, which is different
223 from the data used in the fitting process since $PM_{2.5}$ is not measured every day in all locations.

Formatted: Subscript

Formatted: Subscript

224 4. Results and Discussion

225 We first discuss the surface $PM_{2.5}$ for a few select locations that are impacted by fires
226 followed by the spatial distribution of MODIS AOD and the FRP for August 2018. We then assess
227 the spatial distribution of surface $PM_{2.5}$ from the GWR method. The validation of the GWR method
228 is then discussed. To further demonstrate the impact of the NWUSC fires on $PM_{2.5}$ air quality in
229 the United States, we show the spatial distribution of the difference between August 2018 and
230 August 2011. We further quantify these results for ten US EPA regions.

Formatted: Subscript

Formatted: Subscript

Formatted: Subscript

231 4.1 Descriptive statistics of satellite data and ground measurements

232 The 2018 summertime Canadian wildfires started around the end of July in British
233 Columbia and continued until mid-September. The fires spread rapidly to the south of Canada
234 during August, causing high concentrations of smoke aerosols to drift down to the US and affecting
235 particulate matter air quality significantly. From late July to mid-September, wildfires in the
236 northwest US that burnt forest and grassland also affected air quality. Starting with the Cougar
237 Creek Fire, then Crescent Mountain and Gilbert Fires, different wildfires in in NWUSC caused
238 severe air pollution in various US cities. Figure 2a shows the rapid increase in $PM_{2.5}$ of selected

Formatted: Subscript

239 US cities from July 1st to August 31st, due to the transport of smoke from these wildfires. For all
240 sites, July had low $PM_{2.5}$ concentrations ($<10 \mu g m^{-3}$) and rapidly increases as fire activity
241 increases. Calculating only from the EPA ground observations, the mean $PM_{2.5}$ of the 17 days for
242 the whole US is $13.7 \mu g m^{-3}$ and the mean $PM_{2.5}$ for Washington (WA) is $40.6 \mu g m^{-3}$, which
243 indicates that the PM pollution is concentrated in the northwestern US for these days. This trend
244 is obvious when comparing the mean $PM_{2.5}$ of all US stations (black line with no markers) and the
245 mean $PM_{2.5}$ of all WA stations (grey line with no markers). Ground-level $PM_{2.5}$ reaches its peak
246 between August 17th-21st and daily $PM_{2.5}$ values during this time period far exceeds the 17-day
247 mean $PM_{2.5}$. For example, mean $PM_{2.5}$ in WA on August 20th is $86.75 \mu g m^{-3}$, which is more
248 than two times the 17-day average of this region. On August 19th, Omak which is located in the
249 foothills of the Okanogan Highlands in WA had $PM_{2.5}$ values exceed $250 \mu g m^{-3}$. According to
250 a review of US wildfire caused $PM_{2.5}$ exposures, 24-h mean $PM_{2.5}$ concentrations from wildfires
251 ranged from 8.7 to $121 \mu g m^{-3}$, with a 24 h maximum concentration of $1659 \mu g m^{-3}$ (Navarro et
252 al., 2018).

253 Table 3 shows relevant statistics of 15 states that have at least one daily record of non-
254 attainment of EPA standard ($>35 \mu g m^{-3}$). From the frequency records of non attainment in the
255 17-day period (last column), four states (Montana, Washington, California and Idaho) were
256 consistently affected by the wildfires, and large portion of ground stations in these states were
257 influenced by smoke aerosols. Most of the neighboring states also suffered from short-term but
258 broad air pollution (third column). Noticeable from these records is that the total number of ground
259 stations in some of the highly affected states (such as Idaho) is not sufficient for capturing the
260 smoke. Although there are total 8 EPA stations in Idaho, only two of them have consistent
261 observations during the fire event; the other two stations have no valid observations, and the

Formatted: Subscript

Formatted: Subscript

Formatted: Subscript

Formatted: Subscript

Formatted: Subscript

Formatted: Subscript

Formatted: Subscript

Formatted: Subscript

Formatted: Subscript

Formatted: Subscript

Formatted: Subscript

Formatted: Subscript

Xue, Gupta, Christopher, submitted to [Atmospheric Chemistry and Physics Discussion](#)

262 remaining four stations have only 2~6 observations during the 17-day period. Limited valid data
263 along with unevenly distributed stations makes it hard to quantify smoke pollution in Northwestern
264 US during the fire event period. Therefore, we utilize satellite data to enlarge the spatial coverage
265 and estimate pollution at a finer spatial resolution.

266 The spatial distribution of AOD shown in Figure 2b indicates that the smoke from Canada
267 is concentrated mostly in Northern US states such as WA, Oregon, Idaho, Montana, North Dakota
268 and Minnesota. The black arrow shows the mean 800hPa-level mean wind for 17 days, and the
269 length of the arrow represents the wind speed in ms^{-1} . Also shown in Figure 2b are wind speeds
270 close to the fire sources which are about 4~5 ms^{-1} , and according to the distances and wind
271 directions, it can take approximately 28~36 hours for the smoke to transport southeastward to
272 Washington state. Then the smoke continues to move east to other northern states such as Montana
273 and North Dakota. In addition, the grey circle represents the total fire radiative power (FRP) of
274 every 2.3×3.5-degree box. The reason for not choosing a smaller grid for the FRP is to not clutter
275 Figure 2b with information from small fires. The bigger the circle is, the stronger the fire is in that
276 grid and different sizes and its corresponding FRP values are shown in the lower right corner. It is
277 clear that the strongest fires in 2018 are located in the Tweedsmuir Provincial Park of British
278 Columbia in Canada (53.333N, 126.417W). The four separate lightning-caused wildfires burnt
279 nearly 301,549 hectares of the boreal forest. The total FRP of August 2018 in Canada is about
280 5362 (*1000 MW), while the total FRP of August 2011 in Canada is 48 (* 1000 MW). The 2011
281 fire was relatively weak compared to the 2018 Tweedsmuir Complex fire and we therefore use the
282 2011 air quality data as a baseline to quantify the 2018 fire influence on $\text{PM}_{2.5}$ in the United States.

283 4.2 Model Fitting and validation

Formatted: Subscript

284 The main goal for using GWR model is to help predict the spatial distribution of $PM_{2.5}$ for
285 places with no ground monitors while leveraging the satellite AOD and therefore it is important to
286 ensure that the model is robust. Figure 3a and 3b show the results for 2018 for GWR model fitting
287 for the entire US and the LOOCV models respectively. The color of the scatter plots represents
288 the probability density function (PDF) which calculates the relative likelihood that the observed
289 ground-level $PM_{2.5}$ would equal the predicted value. The lighter the color is, the more points are
290 present, with a higher correlation. The model fitting process estimates the slope for each variable
291 and therefore the model can be fitted close to the observed $PM_{2.5}$ and using this estimated
292 relationship we are able to assess surface $PM_{2.5}$ using other parameters at locations where $PM_{2.5}$
293 monitors are not available. The LOOCV process tests the model performance in predicting $PM_{2.5}$.
294 If the results of LOOCV has a large bias from the model fitting, then the predictability of the model
295 is low. Higher R^2 difference and RMSE difference value indicate that the model is overfitting and
296 not suitable. The R^2 for the model fitting is 0.834, and the R^2 for the LOOCV is 0.797; the RMSE
297 for the GWR model fitting is $3.46 \mu g m^{-3}$, and for LOOCV the RMSE is $3.84 \mu g m^{-3}$. There are
298 minor differences between fitting R^2 and validation R^2 (0.037) and between fitting RMSE and
299 validation RMSE ($0.376 \mu g m^{-3}$) suggesting that the model is not over-fitting and has stable
300 predictability further indicating that the model can predict surface $PM_{2.5}$ reliably. In addition, we
301 also performed a 20-fold cross validation by splitting the dataset into 20 consecutive folds, and
302 each fold is used for validation while the 19 remaining folds form the training set. The 20-fold
303 cross validation has R^2 of 0.745 and RMSE of $4.3 \mu g m^{-3}$. The increase/decrease in the cross
304 validated R^2 and RMSE indicates the importance of sufficient data used for fitting since a small
305 decrease in the number of fitting data can reduce the model prediction accuracy. Overall, the
306 prediction error of the model is between $3\sim 5 \mu g m^{-3}$, which is a reasonable error range for 17-day

Formatted: Subscript

Formatted: Subscript

Formatted: Subscript

Formatted: Subscript

Formatted: Subscript

Formatted: Subscript

Formatted: Subscript

307 average prediction of $PM_{2.5}$. For data greater than the EPA standard ($35 \mu g m^{-3}$), the model has
308 a RMSE of $12.07 \mu g m^{-3}$, which is a lot larger than the RMSE when using the entire model.

309 Therefore, the model has a tendency for underestimating $PM_{2.5}$ exceedances by around 12.07
310 $\mu g m^{-3}$. The larger the $PM_{2.5}$ is, the greater the model underestimates. To examine the model
311 performance for high and low polluted areas, the results are divided into two parts ($PM_{2.5} > 35$
312 $\mu g m^{-3}$ and $PM_{2.5} < 35 \mu g m^{-3}$). has Areas with high pollution have R^2 of 0.64 and areas with
313 low pollution have R^2 of 0.67, therefore, the model performance is relative stable for both large
314 and small $PM_{2.5}$ values.

315 **4.3 Predictors' influence during wildfires**

316 Table 4 shows the GWR model mean coefficients for the whole US region and for different
317 selected regions. The selected boxes are shown in figure 4c in different colors: box1 (red) located in NW
318 US include major fire sources in US; box2 (gold) located in Montana state is influenced from both
319 neighboring states and smoke from Canada; box3 (green) in Minnesota which is located further from the
320 fires and has minor increase in $PM_{2.5}$ due to remote smoke; box4 (black) in NE (Northeast) US is the furthest
321 from fires and has no obvious pollution increase. The second column of the tables shows the conditions for
322 sample selection and the third column shows the number of pixels selected for each box. By comparing the
323 coefficients of samples selected in these boxes, predictors have different influence in different locations.
324 AOD has stronger influence on predicting $PM_{2.5}$ closer to fire sources, but local emissions become more
325 dominant if the distances is large enough. The smoke flag is overall positive related to surface $PM_{2.5}$, while
326 it could slightly negatively relate to $PM_{2.5}$ around fire sources and northeastern coasts. PBL is negatively
327 related to $PM_{2.5}$ when the pollution is concentrated near the surface (fires or human-made emissions), while
328 it appears to be positively related to $PM_{2.5}$ at locations where the main pollution source comes from remote
329 wildfire smoke. Surface temperature have a relative stable positive correlation with surface $PM_{2.5}$, however,
330 surface pressure and wind speeds are negatively correlated with $PM_{2.5}$. Relative humidity, on the other hand,

Formatted: Subscript

Formatted: Subscript

Formatted: Subscript

Deleted: The higher polluted part has

Deleted: the lower part has

Formatted: Font: Bold

Deleted: mean

Deleted: coefficients from the GWR model

Deleted: B

Deleted: Washington state

Deleted: is nearby the

Formatted: Subscript

Deleted: Pennsylvania state

Formatted: Subscript

Formatted: Subscript

Formatted: Subscript

Formatted: Subscript

Formatted: Subscript

Formatted: Subscript

Formatted: Subscript

339 shows large variations on $PM_{2.5}$ influence across the nation. Around the wildfires where the RH is relative
340 low, RH has a positive correlation with $PM_{2.5}$ since hygroscopicity would increase and leads to
341 accumulation of $PM_{2.5}$, but increasing RH can also decrease $PM_{2.5}$ concentration by overgrowing the $PM_{2.5}$
342 particles to deposition at high RH environment (Chen et al., 2018).

343 4.4 Predicted $PM_{2.5}$ Distribution

344 The mean $PM_{2.5}$ distributions over the United States shown in Figure 4a is calculated by
345 averaging the surface $PM_{2.5}$ data from ground monitors for the 17 days, which matches well with
346 the GWR model-predicted $PM_{2.5}$ distributions shown in Figure 4b. The model estimation extends
347 the ground measurements and provide pollution assessments across the entire nation. Comparing
348 the AOD map (Figure 2b) with the $PM_{2.5}$ estimations (Figure 4b), demonstrates the differences
349 between columnar and surface-level pollution. Differences between the AOD and $PM_{2.5}$
350 distributions are due to various reasons including 1) Areas with high $PM_{2.5}$ concentrations in figure
351 4b correspond to low AOD values in figure 2b (Southern California, Utah, and southern US); 2)
352 and high AOD regions in figure 2b correspond to low $PM_{2.5}$ concentrations in figure 4b
353 (Minnesota). The first situation usually occurs at the edge of polluted areas that are relative far
354 from the fire source, which is consistent with previous studies that reported smaller particles (<10
355 μg) are able to travel longer distances compared to large particles ($>10 \mu g$) (Gillies et al., 1996),
356 and that larger particles tend to settle closer to their source (Sapkota et al., 2005; Zhu et al., 2002).

357 We use the same method for August 9th to August 25th in 2011 that had low fire activity,
358 ensuring consistency for estimating coefficients for different variables for 2011. Figure 4c shows
359 the difference in spatial distribution of mean ground $PM_{2.5}$ of the 17 days between 2018 and 2011.
360 High values of $PM_{2.5}$ differences are in the Northwestern and central parts of the United States
361 with the Southern states having very little impact due to the fires. Of all the 48 states within the

Formatted: Subscript

Formatted: Subscript

Formatted: Subscript

Formatted: Subscript

Formatted: Subscript

Formatted: Subscript

Formatted: Subscript

Formatted: Subscript

Formatted: Subscript

Formatted: Subscript

Formatted: Subscript

Formatted: Subscript

Formatted: Subscript

Formatted: Subscript

Formatted: Subscript

Xue, Gupta, Christopher, submitted to [Atmospheric Chemistry and Physics Discussion](#)

362 study region, there are 29 states that have a higher $PM_{2.5}$ value in 2018 than 2011, and 15 states
363 have 2018 $PM_{2.5}$ value more than two times their 2011 value (shown in figure 5). The mean $PM_{2.5}$
364 for WA increases from 5.87 in 2011 to $46.47 \mu g m^{-3}$ in 2018, which is about 8 times more than
365 2011 values. The $PM_{2.5}$ values in Oregon increases from 4.97 (in 2011) to $33.3 \mu g m^{-3}$ in 2018,
366 which is nearly seven times more than in 2011. For states from Montana to Minnesota, the mean
367 $PM_{2.5}$ decreases from east to west, which reveals the path of smoke transport. As shown in Figure
368 4c, there is a clear transport path of smoke from North Dakota all the way to Texas. Along the
369 path, smoke increases $PM_{2.5}$ concentrations by 168% in North Dakota and 27% in Texas. Smoke
370 aerosols transported over long distances contains fine fraction PM which significantly affect the
371 health of children, adults, and vulnerable groups.

372 Figure 5 shows the mean $PM_{2.5}$ predicted from the GWR model of different EPA regions
373 for the 17 days in 2011 and 2018 (Hawaii and Alaska are not included). The most influenced region
374 is region 10, which has a 2018 mean $PM_{2.5}$ value of $34.2 \mu g m^{-3}$ that is 6 times larger than the
375 values in 2011 ($5.8 \mu g m^{-3}$) values. The $PM_{2.5}$ of region 8 and 9 have 2.4 and 2.6 times increase
376 in 2018 compared to 2011. Region 1~4 have lower $PM_{2.5}$ in 2018 than 2011 possibly due to Clean
377 Air Act initiatives, absence of any major fire activities and further away for transported aerosols.
378 The emission reduction improves the US air quality and lower the $PM_{2.5}$ every year, but 6 out of
379 10 EPA regions show significant increases in $PM_{2.5}$ during the study period, which indicates that
380 the long-range transported wildfire smoke has become the new major pollutant in the US.

381 4.5 Estimation of Canadian fire pollution

382 To evaluate the pollution caused only from Canadian fires, we did a rough assessment
383 according to the total FRP and $PM_{2.5}$ values. There are three states in the US have wildfires during
384 the study period: California, Washington and Oregon, and they have total FRP of 1186, 518 and

Formatted: Subscript

Formatted: Subscript

Formatted: Subscript

Formatted: Subscript

Formatted: Subscript

Formatted: Subscript

Formatted: Subscript

Formatted: Subscript

Formatted: Subscript

Formatted: Subscript

Formatted: Subscript

Formatted: Subscript

Formatted: Subscript

Xue, Gupta, Christopher, submitted to [Atmospheric Chemistry and Physics Discussion](#)

385 439 (*1000 MW) respectively. Assuming that California was only influenced by the local fires,
386 then fires of 1186 (*1000 MW) cause $13 \mu\text{g m}^{-3}$ increase in $\text{PM}_{2.5}$. Accordingly, wildfires in
387 Washington and Oregon State will cause 6 and $5 \mu\text{g m}^{-3}$ increase in state mean $\text{PM}_{2.5}$. Therefore,
388 Canadian fires caused $\text{PM}_{2.5}$ increase in Washington and Oregon is about 35 and $23 \mu\text{g m}^{-3}$. Since
389 the FRP of Canadian wildfires are approximately 5 times larger than that of the California fires,
390 which is the strongest fire in US, we assume the pollution affecting the states located in the
391 downwind directions other than the three states are mainly coming from Canadian wildfires. States
392 with no local fires such as Montana, North Dakota, South Dakota and Minnesota have $\text{PM}_{2.5}$
393 increase of 18.31, 12.8, 10.4 and $10.13 \mu\text{g m}^{-3}$. The decrease of these numbers reveal that the
394 smoke is transport in a SE direction. This influence of Canadian wildfires on US air quality is only
395 a rough quantity estimation, thus additional work is needed for understand long-range transport
396 smoke pollution and its impact on public health. One way to do this would be assessing the
397 difference of pollution by turning on and off US fires in chemistry models.

398 4.6 Model uncertainties and limitations

399 There are various sources of uncertainties and limitations for studies that use satellite data
400 to estimate surface $\text{PM}_{2.5}$ concentrations. Since wildfires develop quickly it is important to have
401 continuous observations to capture the rapid changes. This study uses polar orbiting high-quality
402 satellite aerosol products, but the temporal evolution can only be estimated by geostationary data
403 sets. Although satellite observations have excellent spatial coverage, missing data due to cloud
404 cover is a limitation. As discussed in the paper, the prediction error (RMSE) of the model is
405 between $3\sim 5 \mu\text{g m}^{-3}$. The GWR model is largely influenced by the distribution of ground stations,
406 and the prediction error will be different in different places due to unevenly distributed $\text{PM}_{2.5}$
407 stations. For locations that have a dense ground-monitoring distribution, the prediction error will

Formatted: Subscript

Formatted: Subscript

Formatted: Subscript

Formatted: Subscript

Formatted: Subscript

Formatted: Subscript

Xue, Gupta, Christopher, submitted to [Atmospheric Chemistry and Physics Discussion](#)

408 be low, while the prediction error will be relative larger at other places with sparse surface stations.
409 Although there are obvious limitations, complementing surface data with satellite products and
410 meteorological and other ancillary information in a statistical model like the GWR has provided
411 robust results for estimating surface $PM_{2.5}$ from wildfires. We also note that we did not consider
412 some variables used in other studies such as NDVI, forest cover, vegetation type, industrial
413 density, visibility and chemical constituents of smoke particles (Donkelaar et al., 2015; Hu et al.,
414 2013; You et al., 2015; Zou et al., 2016). Visibility mentioned in some studies may improve the
415 model performance, but unlike AOD, it has limited measurement across the nation, which will
416 restrict the applicability of training data. [Another uncertainty comes from the 2011 wildfires which](#)
417 [we assumed to be zero fire events but there are actually few fire events in EPA region 6, 8, 9 and](#)
418 [10, and this will lead to underestimation of \$PM_{2.5}\$ increase due to 2018 fires in these regions.](#)

419 One limitation of this study is that analysis based on 17-day mean values cannot capture
420 daily pollution variations, which is also very important for pollution estimation during rapid-
421 changing wildfire events. To extend this analysis to daily estimation, the cloud contaminations of
422 satellite observations become a major problem. Therefore, future work is needed using chemistry
423 transport models and other data to fill in the gaps on missing AOD data due to cloud coverage.

424 5. Summary and Conclusions

425 We estimate the surface mean $PM_{2.5}$ for 17 days in August for a high fire active year (2018)
426 and compare that with a low fire activity year using the Geographically Weighted Regression
427 (GWR) method to assess the increase in $PM_{2.5}$ in the United States due to smoke transported from
428 fires. The difference in $PM_{2.5}$ between the two years indicates that more than half of the US states
429 (29 states) are influenced by the NWUSC wildfires, and half of the affected states have 17-day
430 mean $PM_{2.5}$ increases larger than 100% of the baseline value. The peak $PM_{2.5}$ during the wildfires

Formatted: Subscript

Formatted: Subscript

Formatted: Subscript

Formatted: Subscript

Formatted: Subscript

Formatted: Subscript

Xue, Gupta, Christopher, submitted to [Atmospheric Chemistry and Physics Discussion](#)

431 can be much larger than the 17-day average and can affect vulnerable populations susceptible to
432 air pollution. Some of the most affected states are in Washington, California, Wisconsin, Colorado
433 and Oregon, all of which have populations greater than 4 million. According to CDC (Centers for
434 Disease Control and Prevention), 8% of the population have asthma (CDC, 2011). Therefore, for
435 asthma alone, there are about 3 million people facing significant health issue due to the long-range
436 transport smoke in these states.

437 For states that show decrease in $PM_{2.5}$ due to the Clean Air Act, the mean decrease is about
438 16% of the baseline after 7 years. This is consistent with EPA's report that there is a 23% decrease
439 of $PM_{2.5}$ in national average from 2010 to 2019 (U.S. Environmental Protection Agency, 2019).

440 Comparing with the dramatic increase (132%) caused by wildfires, pollution from the fires is
441 counteracting our effort on emission controls. Although wildfires are often episodic and short-
442 term, high frequency of fire occurrence and increasing longer durations of summertime wildfires
443 in recent years has made them now a long-term influence on public lives. Our results show a
444 significant increase of pollution in a short time period in most of the US states due to the NWUSC
445 wildfires, which affects millions of people. With wildfires becoming more frequent during recent
446 years, more effort is needed to predict and warn the public about the long-range transported smoke
447 from wildfires.

448 **Acknowledgements.**

449 Pawan Gupta was supported by a NASA Grant. MODIS data were acquired from the Goddard
450 DAAC. We thank all the data providers for making this research possible.

451 **References**

452 Apte, J.S., Brauer, M., Cohen, A.J., Ezzati, M., Pope, C.A., 2018. Ambient $PM_{2.5}$ Reduces

Formatted: Subscript

Formatted: Subscript

Xue, Gupta, Christopher, submitted to [Atmospheric Chemistry and Physics Discussion](#)

453 Global and Regional Life Expectancy. *Environ. Sci. Technol. Lett.* 5, 546–551.

454 <https://doi.org/10.1021/acs.estlett.8b00360>

455 Brunsdon, C., Fotheringham, A.S., Charlton, M.E., 1996. Geographically Weighted Regression:

456 A Method for Exploring Spatial Nonstationarity. *Geogr. Anal.* 28, 281–298.

457 <https://doi.org/https://doi.org/10.1111/j.1538-4632.1996.tb00936.x>

458 Calkin, D.E., Thompson, M.P., Finney, M.A., 2015. Negative consequences of positive

459 feedbacks in us wildfire management. *For. Ecosyst.* 2, 1–10.

460 <https://doi.org/10.1186/s40663-015-0033-8>

461 Cascio, W.E., 2018. Wildland Fire Smoke and Human Health. *Sci. Total Environ.* 624, 586–595.

462 <https://doi.org/10.1016/j.scitotenv.2017.12.086>.

463 CDC, 2011. Asthma in the US. *CDC Vital Signs* 1–4.

464 Chen, D., Xie, X., Zhou, Y., Lang, J., Xu, T., Yang, N., Zhao, Y., Liu, X., 2017. Performance

465 evaluation of the WRF-chem model with different physical parameterization schemes

466 during an extremely high PM_{2.5} pollution episode in Beijing. *Aerosol Air Qual. Res.* 17,

467 262–277. <https://doi.org/10.4209/aaqr.2015.10.0610>

468 Chen, Z., Chen, D., Zhao, C., Kwan, M. po, Cai, J., Zhuang, Y., Zhao, B., Wang, X., Chen, B.,

469 Yang, J., Li, R., He, B., Gao, B., Wang, K., Xu, B., 2020. Influence of meteorological

470 conditions on PM_{2.5} concentrations across China: A review of methodology and

471 mechanism. *Environ. Int.* 139, 105558. <https://doi.org/10.1016/j.envint.2020.105558>

472 Chen, Z., Xie, X., Cai, J., Chen, D., Gao, B., He, B., Cheng, N., Xu, B., 2018. Understanding

473 meteorological influences on PM_{2.5} concentrations across China: A temporal and spatial

Xue, Gupta, Christopher, submitted to [Atmospheric Chemistry and Physics Discussion](#)

474 perspective. *Atmos. Chem. Phys.* 18, 5343–5358. <https://doi.org/10.5194/acp-18-5343-2018>

475 Chu, Y., Liu, Y., Li, X., Liu, Z., Lu, H., Lu, Y., Mao, Z., Chen, X., Li, N., Ren, M., Liu, F., Tian,

476 L., Zhu, Z., Xiang, H., 2016. A review on predicting ground PM_{2.5} concentration using

477 satellite aerosol optical depth. *Atmosphere (Basel)*. 7, 129.

478 <https://doi.org/10.3390/atmos7100129>

479 Coogan, S.C.P., Robinne, F.N., Jain, P., Flannigan, M.D., 2019. Scientists' warning on wildfire

480 — a canadian perspective. *Can. J. For. Res.* 49, 1015–1023. <https://doi.org/10.1139/cjfr->

481 2019-0094

482 Donkelaar, A. Van, Martin, R. V., Li, C., Burnett, R.T., 2019. Regional Estimates of Chemical

483 Composition of Fine Particulate Matter Using a Combined Geoscience-Statistical Method

484 with Information from Satellites, Models, and Monitors. *Environ. Sci. Technol.* 53, 2595–

485 2611. <https://doi.org/10.1021/acs.est.8b06392>

486 Donkelaar, A. Van, Martin, R. V., Park, R.J., 2006. Estimating ground-level PM_{2.5} using

487 aerosol optical depth determined from satellite remote sensing. *J. Geophys. Res. Atmos.*

488 111. <https://doi.org/10.1029/2005JD006996>

489 Donkelaar, A. Van, Martin, R. V., Spurr, R.J.D., Burnett, R.T., 2015. High-Resolution Satellite-

490 Derived PM_{2.5} from Optimal Estimation and Geographically Weighted Regression over

491 North America. *Environ. Sci. Technol.* 49, 10482–10491.

492 <https://doi.org/10.1021/acs.est.5b02076>

493 Dressen, J., Sullivan, J., Delgado, R., 2016. Observations and impacts of transported Canadian

494 wildfire smoke on ozone and aerosol air quality in the Maryland region on June 9–12, 2015.

495 *J. Air Waste Manag. Assoc.* 66, 842–862. <https://doi.org/10.1080/10962247.2016.1161674>

Xue, Gupta, Christopher, submitted to [Atmospheric Chemistry and Physics Discussion](#)

496 Fotheringham, A.S., Charlton, M.E., Brunson, C., 1998. Geographically weighted regression: a
497 natural evolution of the expansion method for spatial data analysis. *Environ. Plan. A* 30,
498 1905–1927.

499 Fotheringham, S.A., Brunson, C., Charlton, M., 2003. *Geographically Weighted Regression :
500 The Analysis of Spatially Varying Relationships*, John Wiley and Sons.

501 Freeborn, P.H., Wooster, M.J., Roy, D.P., Cochrane, M.A., 2014. Quantification of MODIS fire
502 radiative power (FRP) measurement uncertainty for use in satellite-based active fire
503 characterization and biomass burning estimation. *Geophys. Res. Lett.* 41, 1988–1994.
504 <https://doi.org/10.1002/2013GL059086>.

505 Goldberg, D.L., Gupta, P., Wang, K., Jena, C., Zhang, Y., Lu, Z., Streets, D.G., 2019. Using gap-
506 filled MAIAC AOD and WRF-Chem to estimate daily PM_{2.5} concentrations at 1 km
507 resolution in the Eastern United States. *Atmos. Environ.* 199, 443–452.
508 <https://doi.org/10.1016/j.atmosenv.2018.11.049>

509 Gu, Y., 2019. *Estimating PM_{2.5} Concentrations Using 3 km MODIS AOD Products : A Case
510 Study in British Columbia , Canada*. University of Waterloo.

511 Guo, B., Wang, X., Pei, L., Su, Y., Zhang, D., Wang, Y., 2021. Identifying the spatiotemporal
512 dynamic of PM_{2.5} concentrations at multiple scales using geographically and temporally
513 weighted regression model across China during 2015–2018. *Sci. Total Environ.* 751.
514 <https://doi.org/10.1016/j.scitotenv.2020.141765>

515 Gupta, P., Christopher, S.A., 2009a. Particulate matter air quality assessment using integrated
516 surface, satellite, and meteorological products: 2. A neural network approach. *J. Geophys.
517 Res. Atmos.* 114, 1–14. <https://doi.org/10.1029/2008JD011497>

Xue, Gupta, Christopher, submitted to [Atmospheric Chemistry and Physics Discussion](#)

- 518 Gupta, P., Christopher, S.A., 2009b. Particulate matter air quality assessment using integrated
519 surface , satellite , and meteorological products : Multiple regression approach. *J. Geophys.*
520 *Res. Atmos.* 114, 1–13. <https://doi.org/10.1029/2008JD011496>
- 521 Hall, E.S., Kaushik, S.M., Vanderpool, R.W., Duvall, R.M., Beaver, M.R., Long, R.W.,
522 Solomon, P.A., 2013. Intergrating Sensor Monitoring Technology into Current Air
523 Pollution Regulatory Support Paradigm: Practical Considerations. *Am. J. Environ. Eng* 4,
524 147–154. <https://doi.org/10.5923/j.ajee.20140406.02>
- 525 Hessburg, P.F., Churchill, D.J., Larson, A.J., Haugo, R.D., Miller, C., Spies, T.A., North, M.P.,
526 Povak, N.A., Belote, R.T., Singleton, P.H., Gaines, W.L., Keane, R.E., Aplet, G.H.,
527 Stephens, S.L., Morgan, P., Bisson, P.A., Rieman, B.E., Salter, R.B., Reeves, G.H., 2015.
528 Restoring fire-prone Inland Pacific landscapes: seven core principles. *Landsc. Ecol.* 30,
529 1805–1835. <https://doi.org/10.1007/s10980-015-0218-0>
- 530 Hoff, R.M., Christopher, S.A., 2009. Remote Sensing of Particulate Pollution from Space : Have
531 We Reached the Promised Land ? *J. Air Waste Manage. Assoc.* 59, 645–675.
532 <https://doi.org/10.3155/1047-3289.59.6.645>
- 533 Hu, X., Waller, L.A., Al-Hamdan, M.Z., Crosson, W.L., Estes, M.G., Estes, S.M., Quattrochi,
534 D.A., Sarnat, J.A., Liu, Y., 2013. Estimating ground-level PM_{2.5} concentrations in the
535 southeastern U.S. using geographically weighted regression. *Environ. Res.* 121, 1–10.
536 <https://doi.org/10.1016/j.envres.2012.11.003>
- 537 Hu, Z., 2009. Spatial analysis of MODIS aerosol optical depth, PM_{2.5}, and chronic coronary
538 heart disease. *Int. J. Health Geogr.* 8, 1–10. <https://doi.org/10.1186/1476-072X-8-27>
- 539 Hubbell, B.J., Crume, R. V., Evarts, D.M., Cohen, J.M., 2010. Policy Monitor: Regulation and

Xue, Gupta, Christopher, submitted to [Atmospheric Chemistry and Physics Discussion](#)

540 progress under the 1990 Clean Air Act Amendments. *Rev. Environ. Econ. Policy* 4, 122–
541 138. <https://doi.org/10.1093/reep/rep019>

542 Hystad, P., Demers, P.A., Johnson, K.C., Brook, J., Van Donkelaar, A., Lamsal, L., Martin, R.,
543 Brauer, M., 2012. Spatiotemporal air pollution exposure assessment for a Canadian
544 population-based lung cancer case-control study. *Environ. Heal. A Glob. Access Sci.*
545 *Source* 11, 1–22. <https://doi.org/10.1186/1476-069X-11-22>

546 J.A.Gillies, W.G.Nickling, G.H.Mctainsh, 1996. Dust concentration s and particle-size
547 characteristics of an intense dust haze event: inland delta region. *Atmos. Environ.* 30, 1081–
548 1090.

549 Kearns, M., Ron, D., 1999. Algorithmic stability and sanity-check bounds for leave-one-out
550 cross-validation. *Neural Comput.* 11, 1427–1453.
551 <https://doi.org/10.1162/089976699300016304>

552 Koelemeijer, R.B.A., Homan, C.D., Matthijsen, J., 2006. Comparison of spatial and temporal
553 variations of aerosol optical thickness and particulate matter over Europe. *Atmos. Environ.*
554 40, 5304–5315. <https://doi.org/10.1016/j.atmosenv.2006.04.044>

555 Kollanus, V., Tiittanen, P., Niemi, J. V., Lanki, T., 2016. Effects of long-range transported air
556 pollution from vegetation fires on daily mortality and hospital admissions in the Helsinki
557 metropolitan area, Finland. *Environ. Res.* 151, 351–358.
558 <https://doi.org/10.1016/j.envres.2016.08.003>

559 Liu, Y., Sarnat, J.A., Kilaru, V., Jacob, D.J., Koutrakis, P., 2005. Estimating ground-level PM_{2.5}
560 in the eastern United States using satellite remote sensing. *Environ. Sci. Technol.* 39, 3269–
561 3278. <https://doi.org/10.1021/es049352m>

Xue, Gupta, Christopher, submitted to [Atmospheric Chemistry and Physics Discussion](#)

562 Loader, C.R., 1999. BANDWIDTH SELECTION: CLASSICAL OR PLUG-IN? *Ann. Stat.* 27,
563 415–438.

564 Lyapustin, A., Korkin, S., Wang, Y., Quayle, B., Laszlo, I., 2012. Discrimination of biomass
565 burning smoke and clouds in MAIAC algorithm. *Atmos. Chem. Phys.* 12, 9679–9686.
566 <https://doi.org/10.5194/acp-12-9679-2012>

567 Lyapustin, A., Wang, Y., Korkin, S., Huang, D., 2018. MODIS Collection 6 MAIAC Algorithm.
568 *Atmos. Meas. Tech.* 11, 5741–5765. <https://doi.org/10.5194/amt-2018-141>

569 Ma, Z., Hu, X., Huang, L., Bi, J., Liu, Y., 2014. Estimating ground-level PM_{2.5} in china using
570 satellite remote sensing. *Environ. Sci. Technol.* 48, 7436–7444.
571 <https://doi.org/10.1021/es5009399>

572 Meixner, T., Wohlgemuth, P., 2004. Wildfire Impacts on Water Quality. *J. Wildl. Fire* 13, 27–
573 35.

574 Melillo, J.M., Richmond, T., Yohe, G.W., 2014. Climate Change Impacts in the United States.
575 *Third Natl. Clim. Assess.* 52. <https://doi.org/10.7930/J0Z31WJ2>.

576 Miao, Y., Liu, S., Guo, J., Huang, S., Yan, Y., Lou, M., 2018. Unraveling the relationships
577 between boundary layer height and PM_{2.5} pollution in China based on four-year radiosonde
578 measurements. *Environ. Pollut.* 243, 1186–1195.
579 <https://doi.org/10.1016/j.envpol.2018.09.070>

580 Miller, D.J., Sun, K., Zondlo, M.A., Kanter, D., Dubovik, O., Welton, E.J., Winker, D.M.,
581 Ginoux, P., 2011. Assessing boreal forest fire smoke aerosol impacts on U.S. air quality: A
582 case study using multiple data sets. *J. Geophys. Res. Atmos.* 116.

Xue, Gupta, Christopher, submitted to [Atmospheric Chemistry and Physics Discussion](#)

583 <https://doi.org/10.1029/2011JD016170>

584 Mirzaei, M., Bertazzon, S., Couloigner, I., 2018. Modeling Wildfire Smoke Pollution by
585 Integrating Land Use Regression and Remote Sensing Data : Regional Multi-Temporal
586 Estimates for Public Health and Exposure Models. *Atmosphere (Basel)*. 9, 335.

587 <https://doi.org/10.3390/atmos9090335>

588 Munoz-alpizar, R., Pavlovic, R., Moran, M.D., Chen, J., Gravel, S., Henderson, S.B., Sylvain,
589 M., Racine, J., Duhamel, A., Gilbert, S., Beaulieu, P., Landry, H., Davignon, D., Cousineau,
590 S., Bouchet, V., 2017. Multi-Year (2013–2016) PM_{2.5} Wildfire Pollution Exposure over
591 North America as Determined from Operational Air Quality Forecasts. *Atmosphere (Basel)*.
592 8, 179. <https://doi.org/10.3390/atmos8090179>

593 Navarro, K.M., Schweizer, D., Balmes, J.R., Cisneros, R., 2018. A review of community smoke
594 exposure from wildfire compared to prescribed fire in the United States. *Atmosphere*
595 *(Basel)*. 9, 1–11. <https://doi.org/10.3390/atmos9050185>

596 Samet, J.M., 2011. The clean air act and health - A clearer view from 2011. *N. Engl. J. Med.*
597 365, 198–201. <https://doi.org/10.1056/NEJMp1103332>

598 Sapkota, A., Symons, J.M., Kleissl, J., Wang, L., Parlange, M.B., Ondov, J., Breysse, P.N.,
599 Diette, G.B., Eggleston, P.A., Buckley, T.J., 2005. Impact of the 2002 Canadian forest fires
600 on particulate matter air quality in Baltimore City. *Environ. Sci. Technol.* 39, 24–32.
601 <https://doi.org/10.1021/es035311z>

602 Stephens, S.L., 2005. Forest fire causes and extent on United States Forest Service lands. *Int. J.*
603 *Wildl. Fire* 14, 213–222. <https://doi.org/10.1071/WF04006>

Xue, Gupta, Christopher, submitted to [Atmospheric Chemistry and Physics Discussion](#)

- 604 Trueblood, M.B., Lobo, P., Hagen, D.E., Achterberg, S.C., Liu, W., Whitefield, P.D., 2018.
605 Application of a hygroscopicity tandem differential mobility analyzer for characterizing PM
606 emissions in exhaust plumes from an aircraft engine burning conventional and alternative
607 fuels. *Atmos. Chem. Phys.* 18, 17029–17045. <https://doi.org/10.5194/acp-18-17029-2018>
- 608 U.S. Environmental Protection Agency, 2019. Particulate Matter (PM2.5) Trends.
- 609 Wang, H., Shi, G., Tian, M., Zhang, L., Chen, Y., Yang, F., Cao, X., 2017. Aerosol optical
610 properties and chemical composition apportionment in Sichuan Basin, China. *Sci. Total
611 Environ.* 577, 245–257. <https://doi.org/10.1016/j.scitotenv.2016.10.173>
- 612 Xu, T., Song, Y., Liu, M., Cai, X., Zhang, H., Guo, J., Zhu, T., 2019. Temperature inversions in
613 severe polluted days derived from radiosonde data in North China from 2011 to 2016. *Sci.
614 Total Environ.* 647, 1011–1020. <https://doi.org/10.1016/j.scitotenv.2018.08.088>
- 615 You, T., Wu, R., Huang, G., Fan, G., 2017. Regional meteorological patterns for heavy pollution
616 events in Beijing. *J. Meteorol. Res.* 31, 597–611. <https://doi.org/10.1007/s13351-017-6143-1>
617 1
- 618 You, W., Zang, Z., Pan, X., Zhang, L., Chen, D., 2015. Estimating PM2.5 in Xi'an, China using
619 aerosol optical depth: A comparison between the MODIS and MISR retrieval models. *Sci.
620 Total Environ.* 505, 1156–1165. <https://doi.org/10.1016/j.scitotenv.2014.11.024>
- 621 You, W., Zang, Z., Zhang, L., Li, Y., Pan, X., Wang, W., 2016. National-scale estimates of
622 ground-level PM2.5 concentration in China using geographically weighted regression based
623 on 3 km resolution MODIS AOD. *Remote Sens.* 8. <https://doi.org/10.3390/rs8030184>
- 624 Zhang, H., Hoff, R.M., Engel-Cox, J.A., 2009. The relation between moderate resolution

Xue, Gupta, Christopher, submitted to [Atmospheric Chemistry and Physics Discussion](#)

625 imaging spectroradiometer (MODIS) aerosol optical depth and PM_{2.5} over the United
626 States: A geographical comparison by U.S. Environmental Protection Agency regions. *J.*
627 *Air Waste Manag. Assoc.* 59, 1358–1369. <https://doi.org/10.3155/1047-3289.59.11.1358>

628 Zhang, H., Wang, Y., Hu, J., Ying, Q., Hu, X.M., 2015. Relationships between meteorological
629 parameters and criteria air pollutants in three megacities in China. *Environ. Res.* 140, 242–
630 254. <https://doi.org/10.1016/j.envres.2015.04.004>

631 Zheng, C., Zhao, C., Zhu, Y., Wang, Y., Shi, X., Wu, X., Chen, T., Wu, F., Qiu, Y., 2017.
632 Analysis of influential factors for the relationship between PM_{2.5} and AOD in Beijing.
633 *Atmos. Chem. Phys.* 17, 13473–13489. <https://doi.org/10.5194/acp-17-13473-2017>

634 Zhu, Y., Hinds, W.C., Kim, S., Sioutas, C., 2002. Concentration and size distribution of ultrafine
635 particles near a major highway. *J. Air Waste Manag. Assoc.* 52, 1032–1042.
636 <https://doi.org/10.1080/10473289.2002.10470842>

637 Zou, B., Pu, Q., Bilal, M., Weng, Q., Zhai, L., Nichol, J.E., 2016. High-resolution Satellite
638 Mapping of Fine Particulates Based on Geographically Weighted Regression. *Ieee Geosci.*
639 *Remote Sens. Lett.* 13, 495–499.

640

641

642

643 Table 1. Datasets used in the study with sources.

644

	Data /Model	Sensor	Spatial Resolution	Temporal Resolution	Accuracy
1	Surface PM _{2.5}	TEOM	Point data	daily	±5~10%
2	Mid visible aerosol optical depth (AOD)	MAIAC_ MODIS	1km	daily	66% compared to AERONET
3	Fire Radiative Power (FRP)	Terra/Aqua- MODIS	1km	daily	± 7%
4	ECMWF (Meteorological variables)		0.25 degree	hourly	

Formatted: Subscript

645 1) <https://www.epa.gov/outdoor-air-quality-data>

646 2) <https://earthdata.nasa.gov/>

647 3) <https://earthdata.nasa.gov/>

648 4) <https://www.ecmwf.int/en/forecasts>

649

650

651

652 Table 2. Total FRP in Canada and Northwestern US in August of Different Years (unit: 10⁴

653 MW)

Year	2010	2011	2012	2013	2014	2015	2016	2017	2018
CA	148.24	4.84	19.93	70.54	107.78	10.39	4.6	307.3	542.99
NW US	16.41	42.84	320.39	192.06	67.01	339.58	112.9	195.64	296.91

654

655 Table 3. statistics of 15 states that violate EPA standards (35 $\mu\text{g m}^{-3}$) during the 17-day wildfire
656 period

State	number of site violate standard	number of site in the state	Percentage of site violate standard (%)	number of days violate standard
Montana	14	15	93.34	16
Washington	18	20	90	16
Oregon	12	14	85.71	5
North Dakota	7	11	63.63	4
Idaho	5	8	62.5	8
Colorado	11	21	52.38	2
South Dakota	5	10	50	1
California	57	119	47.9	14
Utah	7	15	46.67	4
Nevada	4	13	30.77	1
Wyoming	7	24	29.2	2
Minnesota	4	26	15.4	2
Texas	3	37	8.1	1
Louisiana	1	14	7.1	1
Arizona	1	20	5	1

657

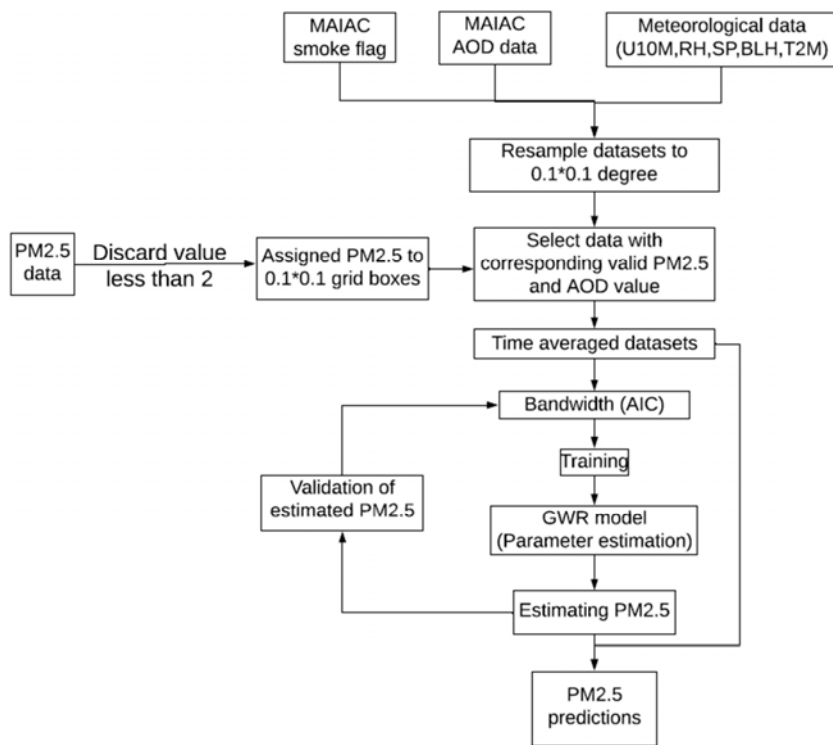
658 Table 4. Coefficients of different predictors

	AOD	Smoke flag	PBL	T2M	RH	U	SP
box1(red)	92.01	-0.13	-1.5	0.2	-0.01	-1.6	-0.037
box2(gold)	63.97	0.002	-2.86	0.09	-0.11	-1.5	-0.02
box3(green)	5.9	0.044	0.3	0.16	0.017	-0.2	-0.015
box4(black)	6.72	-0.02	-1.3	0.28	-0.03	0.13	-0.007
mean	28.1	0.02	-0.89	0.06	-0.19	-0.67	-0.002

659

660

661



662

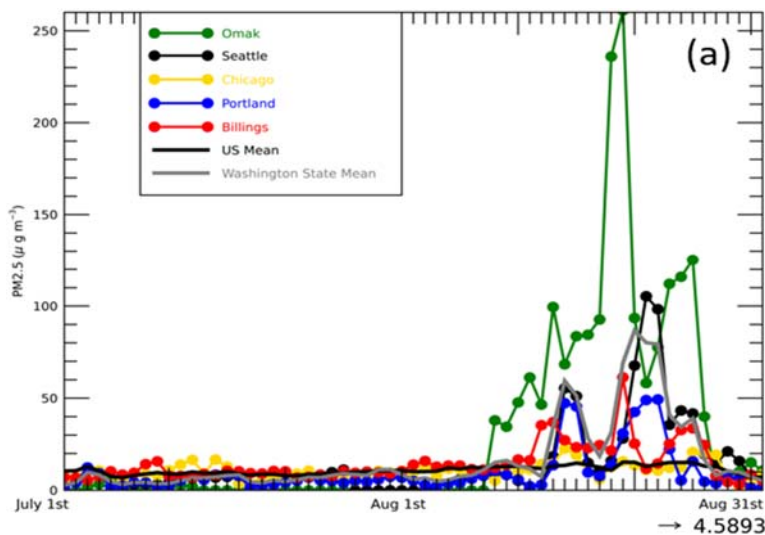
663 Figure 1. Flow chart for the Geographically Weighted Regression model used. All satellite,

664

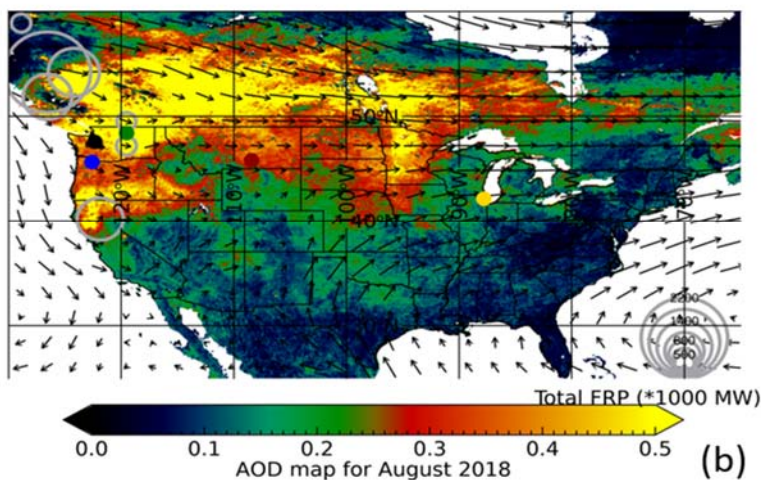
ground, meteorological data are gridded to 0.1 by 0.1 degrees.

665

666



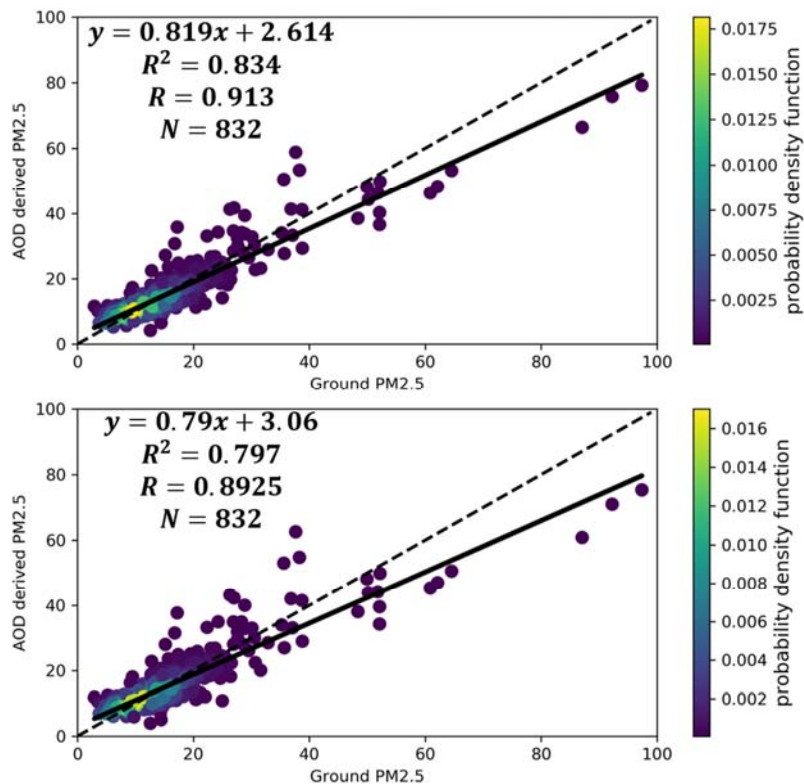
667



668

669 Figure 2. (a) Variations of EPA ground observed PM_{2.5} in different cities from July to August
670 2018 (Omak-Washington, Seattle-Washington, Chicago-Illinois, Portland-Oregon, Billings-
671 Montana). Black line without markers shows the mean variation of the whole US stations and the
672 grey line without markers shows the mean variation of stations in Washington state. (b) Mean
673 MAIAC satellite AOD distribution from August 9th to August 25th, 2018. AOD values equal or
674 larger than 0.5 are shown as the same color (yellow). Also shown are circles with Fire Radiative
675 Power (FRP). Black arrow shows the wind direction and the length of it represents the wind
676 speed. The round spots of different colors on the map show the locations of the five selected
677 cities (green-Omak, black-Seattle, yellow-Chicago, blue-Portland, red-Billings).

Formatted: Subscript



678

679 Figure 3. Results of model fitting and cross validation for GWR model for the entire US region
680 averaged from August 9th to August 25th, 2018. (a) GWR model fitting results (b) GWR model
681 LOOCV results. The dash line is the 1:1 line as reference and the black line shows the regression
682 line. The color of the scatter plots represents the probability density function which provides a
683 relative likelihood that the value of the random variable would equal a certain sample.

684

685

686

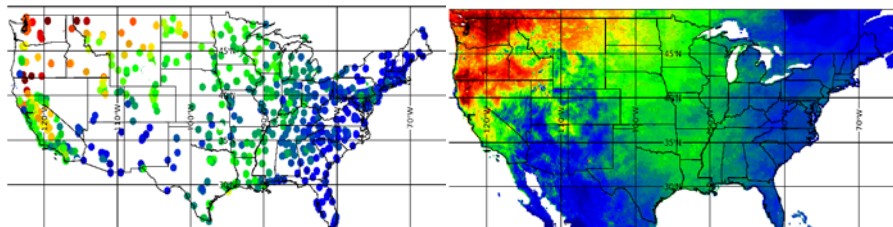
687

688

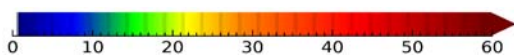
689

690

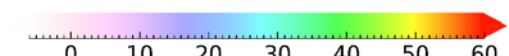
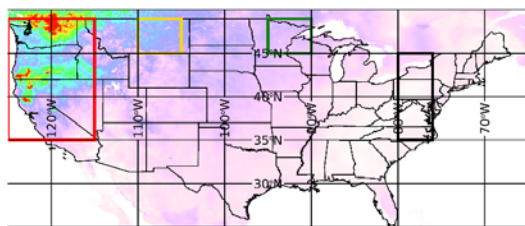
691



692



693



D-PM2.5 map between 2018 and 2011 August

694

Figure 4. (a) EPA ground observed $PM_{2.5}$ distribution over the US averaged from August 9th to August 25th, 2018. (b) GWR predicted 17-day mean $PM_{2.5}$ distribution. (c) Difference map of predicted ground $PM_{2.5}$ of the 17-day mean values between 2018 and 2011. $PM_{2.5}$ values equal or larger than $60 \mu g m^{-3}$ are shown as the same color (red). Note that the D- $PM_{2.5}$ has a different color scale to make the negative values more apparent (blue).

695

696

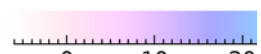
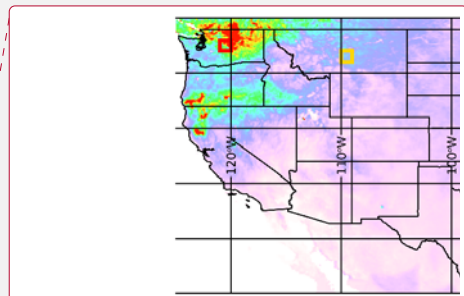
697

698

699

700

701



D-PM2.5 map between 2018 and 2011 August

Deleted:

Formatted: Subscript

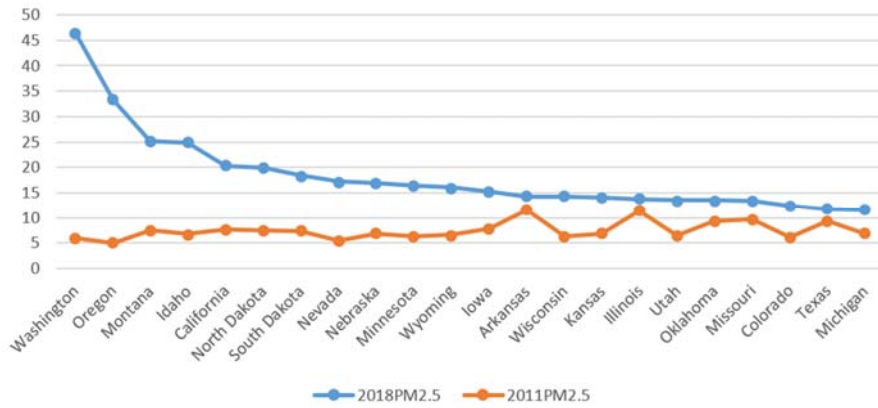
Formatted: Subscript

Formatted: Subscript

Formatted: Subscript

Deleted: 3

Formatted: Subscript



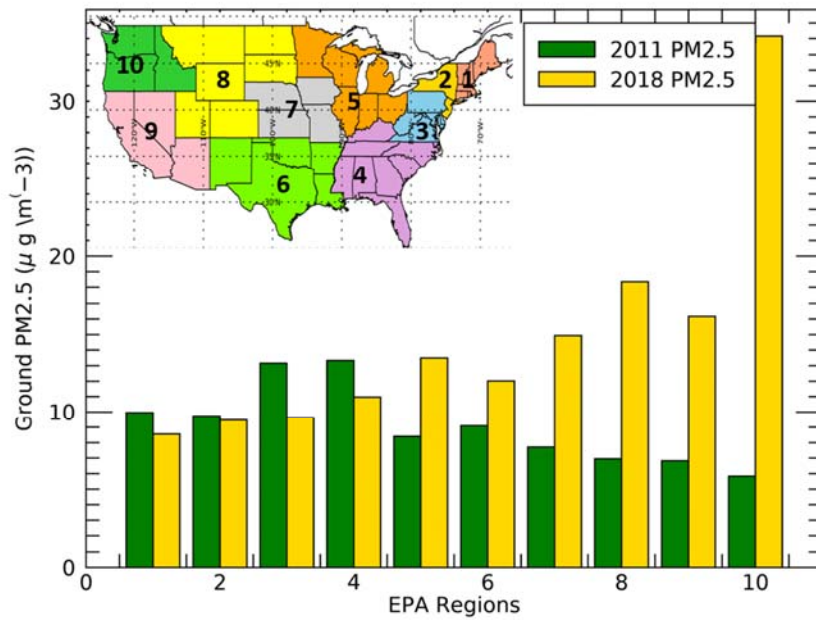
704

705

706

Figure 5. Mean PM_{2.5} from August 9th to August 25th in 2018 and 2011 of most affected states

Formatted: Subscript



707

708 Figure 6. Mean $PM_{2.5}$ of EPA regions from August 9th to August 25th in 2011 and 2018. Inset
709 shows the map of 10 EPA regions in different colors. Yellow column represents the 2018 mean
710 $PM_{2.5}$ and green column represents for 2011 mean $PM_{2.5}$.

711

712

Formatted: Subscript

Formatted: Subscript

Formatted: Subscript